Azimuthal auroral expansion associated with fast flows in the near-Earth plasma sheet: Coordinated observations of the THEMIS all-sky imagers and multiple spacecraft

K. Ogasawara,[1] Y. Kasaba,[1] Y. Nishimura,[2,3] T. Hori,[2] T. Takada,[4] Y. Miyashita,[2] V. Angelopoulos,[5] S. B. Mende,[6] and J. Bonnell[6]

Received 19 August 2010; revised 1 March 2011; accepted 9 March 2011; published 11 June 2011.

[1] Fast azimuthal auroral expansion and poleward expansion are characteristic features of the expansion phase of substorms. In the first study of its kind, we have investigated the azimuthal auroral expansion and its magnetospheric counterpart using data from Time History of Events and Macroscale Interactions during Substorms (THEMIS) all-sky imagers and multiple spacecraft. During the tail season in 2008–2009, we found 16 events of azimuthally expanding aurora that passed near the magnetic footprints of the multiple spacecraft operating in the near-Earth plasma sheet. In the magnetosphere, these events commonly showed fast azimuthal and earthward flows associated with intense electric fields and magnetic dipolarization. The speed of the propagating structure, which was estimated from the time difference of the depolarization observed by the multiple spacecraft, was close to the measured azimuthal plasma flow velocity. We also found that this azimuthal plasma transport was dominated by the **E** × **B** drift speed associated with the enhanced electric field. In a statistical analysis, the averaged speeds of the leading edge of the westward and eastward auroral expansion were 8.8 and 5.3 km/s, respectively. When mapped onto the equatorial magnetosphere, these speeds (267 and 162 km/s) were comparable to the averaged azimuthal plasma (**E** × **B**) flow speeds observed by the spacecraft, which were 193 (239) km/s in the westward direction and 112 (139) km/s in the eastward direction. Our events showed that **E** × **B** flows and auroral expansion predominantly propagated westward, indicating an effect of westward background convection in the Harang flow shear. From these results, we concluded that the azimuthal auroral expansion was closely related to magnetic dipolarization which expanded azimuthally at the **E** × **B** drift speed. On the basis of the abrupt formation of the fast **E** × **B** flows and their propagation away from the onset location, we suggest that the effects of the intense large-scale electric fields, which are possibly generated through substorm onset turbulence, propagate to the ionosphere along the magnetic field lines and lead to azimuthal expansion of an auroral arc.

Citation: Ogasawara, K., Y. Kasaba, Y. Nishimura, T. Hori, T. Takada, Y. Miyashita, V. Angelopoulos, S. B. Mende, and J. Bonnell (2011), Azimuthal auroral expansion associated with fast flows in the near-Earth plasma sheet: Coordinated observations of the THEMIS all-sky imagers and multiple spacecraft, *J. Geophys. Res.*, *116*, A06209, doi:10.1029/2010JA016032.

1. Introduction

[2] Substorms are energy storage and abrupt release processes in the magnetosphere-ionosphere coupled system associated with the reconfiguration of the magnetosphere and auroral illumination. The substorm expansion phase is characterized by magnetic dipolarization, which expands azimuthally and radially from an initially small region at $X \approx -7$ to $-10\ R_E$ in the near-Earth plasma sheet [e.g., *Lopez et al.*, 1990; *Miyashita et al.*, 2009] and by azimuthal and poleward auroral expansion in the ionosphere [e.g., *Akasofu*, 1964; *Oguti*, 1973; *Nakamura et al.*, 1993]. These phenomena are considered to be a consequence of near-Earth instabilities such as the ballooning instability with a periodic wavy structure as suggested in the current disruption model [e.g., *Lui*, 1996; *Liang et al.*, 2005, 2008]. The braking of a fast

[1]Department of Geophysics, Tohoku University, Sendai, Japan.
[2]Solar-Terrestrial Environment Laboratory, Nagoya University, Nagoya, Japan.
[3]Department of Atmospheric and Oceanic Sciences, University of California, Los Angeles, California, USA.
[4]Department of Electrical Engineering and Information Science, Kochi National College of Technology, Kochi, Japan.
[5]Institute of Geophysics and Planetary Physics, University of California, Los Angeles, California, USA.
[6]Space Sciences Laboratory, University of California, Berkeley, California, USA.

0148-0227/11/2010JA016032

earthward flow propagating from the midtail could also lead to substorm expansion (near-Earth neutral line model) [e.g., *Shiokawa et al.*, 1997, 1998]. Particularly, recent Time History of Events and Macroscale Interactions during Substorms (THEMIS) spacecraft and imager observations suggest the importance of such flow bursts leading to substorm expansion onset [*Angelopoulos et al.*, 2008a; *Nishimura et al.*, 2010]. While these expansion phase phenomena are well documented, the direct relationship between an expanding aurora and its magnetospheric counterpart has not yet been fully examined because of the lack of detailed investigations of ground-space conjunctions close to the onset locations.

[3] Several previous studies have examined auroral expansion associated with magnetic dipolarization. For example, by examining the GOES spacecraft and Polar Ultraviolet Imager global images, *Liou et al.* [2002] showed that the auroral bulge was closely associated with magnetic dipolarization and concluded that the dipolarization region expanded westward, eastward, and earthward at the geosynchronous altitude during the auroral expansion. However, the mechanism of the expansion could not be determined since the GOES spacecraft observed magnetic fields only in the region far from the onset location. In addition, the auroral global imager lacked the temporal resolution necessary to resolve the fast auroral expansion feature.

[4] Several possibilities have been considered as corresponding magnetospheric signatures of auroral expansion: wave propagation, $\mathbf{E} \times \mathbf{B}$ drifts, and non-MHD processes such as pressure gradient–related flows. *Uritsky et al.* [2009] suggested that the azimuthally propagating arc wave prior to substorm onset was an auroral footprint of the drift wave mode in the stretched magnetotail. The same process might be expected to work during the expansion phase, leading to auroral expansion. On the other hand, intense electric fields are known to be associated with dipolarization during the substorm expansion phase [*Birn and Hesse*, 1996; *Tu et al.*, 2000; *Ohtani et al.*, 2007; *Nishimura et al.*, 2008], although it is not clear how these electric fields are related to the auroral expansion. To determine the contributions of these processes, it is necessary to perform conjunction studies of the auroral expansion and in situ magnetospheric field and particle measurements near the onset region. Moreover, auroral passages near the magnetic footprints of spacecraft should be detected with a high spatial and temporal resolution.

[5] The capability of the THEMIS project, with its combination of global auroral imaging by the all-sky imager (ASI) array [*Mende et al.*, 2008] and in situ measurements performed by multiple spacecraft [*Angelopoulos*, 2008], provides the first opportunity to address these issues. Using this advantage, *Shiokawa et al.* [2009] reported a faint eastward extension of an auroral arc from the onset location by utilizing the capabilities of the THEMIS spacecraft and ASIs. Shiokawa et al. suggested that this faint extension was associated with earthward flow braking processes and pileup of dipolelike fields in the near-Earth plasma sheet. However, in the event that they studied, the spacecraft were located more than 2.0 h magnetic local time (MLT) away from the onset location; therefore, the azimuthally expanding aurora did not reach the spacecraft meridian. Thus, the magnetospheric feature directly related to auroral expansion has not yet been detected.

[6] In the present paper, we focus on the azimuthal expansion of an auroral arc just after auroral breakup; this expansion was captured by the THEMIS ASIs and multiple spacecraft as it passed the magnetic footprints of the spacecraft. Poleward auroral expansion has not been addressed here because it is not easy to do precise mapping in the meridional direction between ionospheric auroral arcs and spacecraft in the magnetosphere under a drastically changing magnetic field configuration associated with magnetic dipolarization. Mapping uncertainties in the azimuthal direction are, on the other hand, expected to be smaller than those in the meridional direction [*Kubyshkina et al.*, 2009]. From the THEMIS observations, we have identified the direct relationship between the azimuthal auroral expansion in the ionosphere and the in situ plasma flows and dipolarization in the near-Earth plasma sheet.

2. Data Sets

[7] The THEMIS probes allow for multipoint observations of fields and particles in the plasma sheet near the equator. In the 2008 season, the apogees of five identical spacecraft were located at ~9 R_E (THEMIS A), ~12 R_E (THEMIS D and E), ~19 R_E (THEMIS C), and ~30 R_E (THEMIS B). The apogee of THEMIS A was shifted to ~12 R_E and was against the plasma sheet in the 2009 season. We used the data of the electric field instrument [*Bonnell et al.*, 2008], the fluxgate magnetometer [*Auster et al.*, 2008], the electrostatic analyzer (ESA) [*McFadden et al.*, 2008], and the solid state telescope (SST). These data are given in a 3 s time resolution. The third component of the electric field is estimated with an assumption of $\mathbf{E} \times \mathbf{B} = 0$. We used this assumption when the inclination of magnetic fields relative to the spin plane was greater than 10°. ESA and SST data are combined in the moment calculation, where SST data are used for particles below 450 keV in order to avoid the large uncertainty arising because of insufficient calibration.

[8] Coordinated ASI observations provide a global coverage of auroras with a high spatial (~1 km near zenith) and temporal (3 s) resolution. The white light imagers cover a wide wavelength band of about 400–700 nm, and images were projected on an ionospheric altitude of 110 km. We also used ground magnetometer data with a 0.5 s time resolution.

[9] A substorm expansion phase typically lasts for a few tens of minutes and sometimes has multiple onsets with 15–20 min intervals [e.g., *Pytte et al.*, 1976], resulting in a global development of auroral bulge. The global development (a few hours MLT) of substorms has been observed at the geosynchronous orbit [e.g., *Nagai*, 1982; *Nagai et al.*, 1983]. In this study, we analyzed, via THEMIS ASIs, the azimuthal expansion of auroral arcs that occurred within the first few minutes of the substorm expansion phase; this expansion passed near the magnetic footprint of the multiple THEMIS spacecraft. While we focused not on the global development of substorms but instead on the initial development with rather short scales (a few minutes and a few tenths of an hour MLT), it is suggested that the near-Earth disturbances in the present study should relate to the formation of the substorm current wedge investigated previously [e.g., *McPherron et al.*, 1973].

[10] In order to detect azimuthal auroral expansion associated with magnetic dipolarization in the near-Earth plasma

Table 1. Azimuthal Auroral Expansion Events[a]

Event	Onset Time (UT)	Onset MLT (h)	Speed of Azimuthal Auroral Expansion Near the TH-D Footprint (Mapped Velocity Onto the Equatorial Magnetosphere) (km/s)	Speed of Azimuthal Auroral Expansion Near the TH-E Footprint (Mapped Velocity Onto the Equatorial Magnetosphere) (km/s)	Spacecraft (MLT at the Footprint (h))	Azimuthal Plasma ($\mathbf{E} \times \mathbf{B}$) Flow Speed Obtained by TH-D (km/s)	Azimuthal Plasma ($\mathbf{E} \times \mathbf{B}$) Flow Speed Obtained by TH-E (km/s)
2008/01/26	1020:00–1030:00	–	−5.3 (−167)	−6.4 (−202)	D (1.7), E (1.4)	−113 (−131)	−125 (−148)
2008/02/05	1208:30	24.3	−9.5 (−246)	−7.3 (−211)	D (1.3), E (0.9)	−53 (−56)	−101 (−103)
2008/02/26	0403:42	22.2	6.4 (235)	5.6 (196)	D (22.1), E (21.8)	294 (309)	272 (185)
2008/02/27	0244:18	21.3	12.7 (408)	12.7 (383)	D (21.7), E (21.4)	305 (706)	461 (544)
2008/03/02	0700:00	25.0	9.5 (307)	9.5 (304)	D (23.0), E (22.7)	163 (172)	181 (230)
2008/03/03	0804:30	22.8	−4.9 (−149)	−5.6 (−171)	D (23.2), E (22.9)	−101 (−198)	−105 (−131)
2008/03/11	0554:00	24.1	12.7 (405)	12.7 (400)	D (22.2), E (21.9)	168 (439)	235 (324)
2008/03/27	0729:18	20.8	11.9 (293)	7.9 (201)	D (21.9), E (21.6)	170 (208)	124 (104)
2008/03/30	0628:30	23.5	5.8 (166)	3.2 (93)	D (21.6), E (21.3)	205 (289)	183 (160)
2009/02/22	0815:00–0825:00	–	−2.7 (−94)	−2.1 (−72)	D (24.9), E (24.6)	−186 (−120)	−202 (−183)
2009/02/28	0536:12	23.5	−4.5 (−153)	6.4 (−203)	D (23.8), E (23.5)	−124 (−159)	−180 (−271)
2009/03/14a	0130:00–0140:00	–	–	10.6 (296)	E (22.6)	–	99 (123)
2009/03/14b	0400:00–0410:00	–	8.0 (247)	6.4 (188)	D (22.8), E (22.5)	80 (128)	115 (29)
2009/03/14c	0506:00	23.4	–	9.5 (310)	E (22.9)	–	131 (154)
2009/03/23	0603:40	22.9	−4.2 (−143)	−4.2 (−139)	D (23.2), E (22.9)	−134 (−111)	−83 (−87)
2009/03/23	0603:40	22.9	8.5 (285)	8.5 (277)	D (23.2), E (22.9)	213 (179)	192 (124)
2009/04/14	0900:00–0910:00	–	8.0 (157)	8.0 (198)	D (22.8), E (22.6)	117 (126)	151 (239)

[a]Shown are onset times, onset MLTs, speeds of azimuthal auroral expansion (as well as velocities mapped onto the equatorial magnetosphere), spacecraft we used (as well as their MLTs at the footprints), and azimuthal plasma (as well as $\mathbf{E} \times \mathbf{B}$ drift) flow speeds obtained by THEMIS D and E. The substorm onset times were defined as initiation of auroral expansion, and the onset times and locations are estimated using both ASIs and ground magnetometer data. Some events showed precedent small auroral intensifications close to the expanded aurora a few minutes prior to the identified onset times, which may be regarded as initial brightening of substorm expansion. In five cases (2008/01/26, 2009/02/22, 2009/03/14a, 2009/03/14b, and 2009/04/14) that have a range of onset times, the onset time could not be unambiguously determined because of the limited fields of view of ASIs. In addition, there are two cases (2009/03/14a and 2009/03/14c) where in situ data from only one spacecraft were used because this footprint alone was located close to the expanding aurora.

sheet, the following three criteria from the THEMIS data sets during the tail season in 2008–2009 were used for event selection:

[11] 1. The auroral images show azimuthal auroral expansion within the first few minutes of the substorm expansion phase.

[12] 2. Azimuthally expanding auroras pass near at least one of the footprints of the multiple THEMIS spacecraft.

[13] 3. The probe selected according to the above criteria observes magnetic dipolarization near the center of the plasma sheet ($\beta > 1$). By our definition, magnetic dipolarization is a steplike increase in B_Z associated with a steplike decrease in $|B_X|$ in the near-Earth plasma sheet, which indicates a drastic reconfiguration of the magnetosphere.

[14] Here, the substorm expansion phase is identified as an abrupt intensification of an auroral arc near the equatorward boundary of the auroral oval followed by poleward expansion [*Akasofu*, 1964] associated with a development of magnetic bays at ground stations near the onset location. We regarded the magnetic bay as the decrease in the X component of ground magnetic fields more than a few tens of nT near the onset location. Although this threshold is rather small compared to past studies, the magnitude of substorms is not significant in this study. We have used in situ data from the THEMIS D and E spacecraft, which had an advantage in detecting azimuthal propagations because these spacecraft essentially have the same orbit separated azimuthally near the apogee. In order to detect magnetic dipolarization in the near-Earth plasma sheet, it is necessary that B_Z increases by 5 nT/min, that its signature is associated with an increase in a magnetic inclination, and that these levels do not return to the initial background level ~10 min after the increases.

[15] During the tail seasons in 2008 and 2009, we found 16 events satisfying these criteria. In these events, azimuthally expanding auroras showed westward (10 events), eastward (5 events), and both westward and eastward (1 event) auroral expansion near the footprints. Concerning the first 15 cases, while eastward (westward) expansion occurred in the identified westward (eastward) expansion cases, such expansion did not reach the spacecraft footprints. On the basis of our conjunction event survey, we think that onset arcs generally expanded both westward and eastward after substorm onset, with westward auroral expansion tending to be more remarkable than eastward expansion in the spatial and temporal scales. However, we have focused only on notable azimuthal expansion events, and we did not count the number of events that did not show significant azimuthal expansion. *Nishimura et al.* [2010] listed 249 auroral breakup events during the tail season in 2008 (145 events of full substorms and 104 events of pseudobreakups); the number of events in the present study was significantly low compared to the results of *Nishimura et al.* [2010]. The small number of events is the result of our requiring two spacecraft conjunctions close to the onset location (event selection criteria 1 and 2). We also require (event selection criterion 3) that the THEMIS spacecraft be located in the central plasma sheet ($\beta > 1$). These severe criteria significantly reduce the number of conjunctions.

[16] Table 1 lists the azimuthal auroral expansion events. In this study, we have defined substorm onset times as the initiation of the auroral expansion that corresponded to a development of magnetic bays at ground stations using both ASI and ground magnetometer data. In five cases that have a range of onset times, the onset times and locations could not be unambiguously determined because of the limited fields

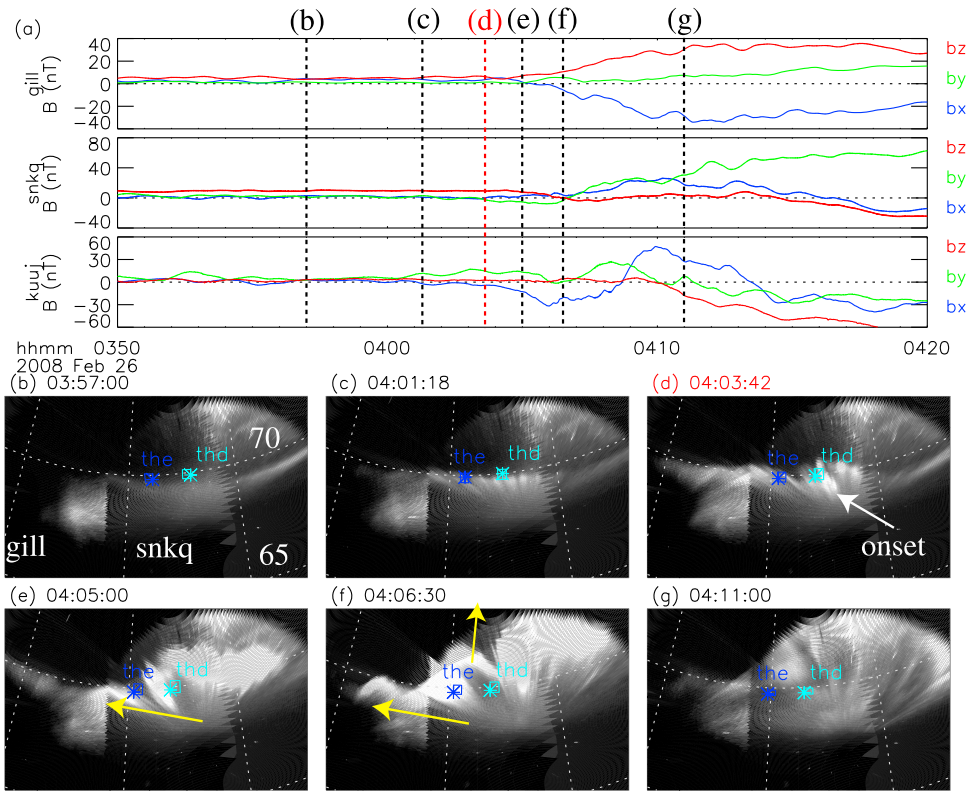

Figure 1. Westward auroral expansion observed by the ground-based instruments on 26 February 2008. (a) Ground magnetometer data near the footprints of THEMIS D and E. (b–g) Sequence of ASI images at the times of the vertical lines shown in Figure 1a. White dashed lines are isocontours of MLAT (every 5°) and MLON (every 15°). All plots cover the magnetic latitudes in the range of ~65°–73° in the premidnight sector of ~20.5–23.5 h MLT. The light blue and blue symbols are the footprints of THEMIS D and E, respectively, mapped by the Tsyganenko 96 model with OMNI solar wind data as input (thd, THEMIS D; the, THEMIS E). In each footprint, time shift errors of ±20 min for the solar wind arrival are shown by the size of the squares. The yellow arrows indicate the directions of auroral expansion. The enhanced brightness commonly appearing in Figures 1b–1g is light contamination.

of view of ASIs. There were two cases where in situ data were used from only one spacecraft because this footprint alone was located close to the expanding aurora. While we have chosen the events where auroral activity was low prior to the auroral expansion, some events showed precedent small auroral intensifications close to the expanded aurora a few minutes prior to the identified onset times, which may be regarded as the initial brightening of a substorm expansion. Moreover, we have not distinguished isolated and multiple-onset substorms. These do not affect our conclusion, however, because we have focused not on the onset mechanism or precise onset timing but rather on the auroral and magnetospheric dynamics during the expansion phase. It should be noted that this study does not require exact footprint positions but rather uses them to roughly estimate the spacecraft meridian relative to the onset meridian. We have also allowed for an error margin of ±20 min in the OMNI solar wind arrival time.

3. Case Studies

[17] In this section, we present two cases that show westward (26 February 2008) and eastward (3 March 2008) auroral expansion near the footprints of the THEMIS spacecraft. In these events, an entire sequence of auroral expansion is detected inside the fields of view of ASIs, and one can easily associate the magnetospheric counterpart with auroral expansion. The fundamental characteristics are generally common in all 16 events.

3.1. The Westward Expansion on 26 February 2008

[18] Figure 1 presents the westward auroral expansion event associated with the auroral onset at 0403:42 UT on 26 February 2008. This event was also examined by *Pu et al.* [2010], who focused on the relationship between magnetic reconnection in the magnetotail and substorm onset using the same ASI data along with four THEMIS probes (B, C, D, and E). The entire sequence of images is given in auxiliary material Animation S1.[1] Figure 1a shows the ground magnetometer data from the Gillam (GILL), Sanikiluaq (SNKQ), and Kuujjuarapik (KUUJ) magnetometers. Figures 1b–1g show a sequence of ASI images obtained at GILL and SNKQ. Each vertical line in Figure 1a marks the time of ASI images shown in Figures 1b–1g. In Figures 1b–1g, the light blue and blue asterisks indicate the

[1] Auxiliary materials are available in the HTML. doi:10.1029/2010JA016032.

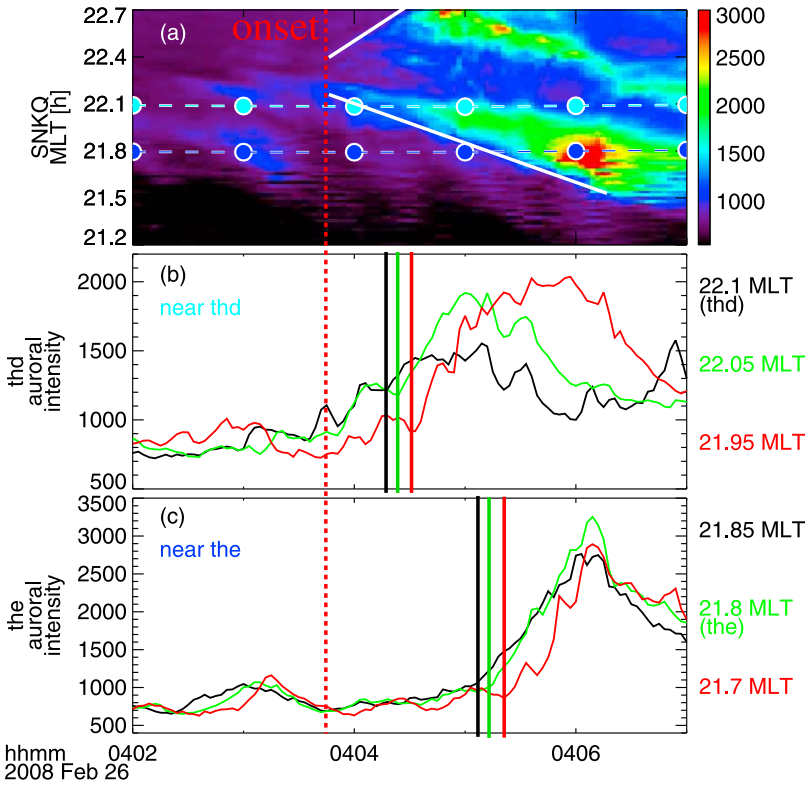

Figure 2. (a) East–west keogram at SNKQ. The footprints of THEMIS D (22.1 h MLT, light blue) and E (21.8 h MLT, blue) are overplotted. The white solid lines indicate the identified leading edges of the azimuthally propagating aurora. (b) Line plots of auroral intensity at different MLTs near the footprint of THEMIS D. The vertical solid lines mark the arrival of the leading edge at each MLT (21.95 h MLT, red; 22.05 h MLT, green; and 22.1 h MLT, black). (c) Same near the footprint of THEMIS E. Red, green, and black lines are for 21.7, 21.8, and 21.85 h MLT, respectively. The vertical red dashed line marks the auroral onset to the east of the footprint of THEMIS D.

footprints of THEMIS D and E, respectively, mapped using the Tsyganenko 96 model [*Tsyganenko*, 1995]. The size of the square of each footprint represents the area where the footprints could possibly move as determined by the error of solar wind arrival.

[19] There were two auroral intensifications around the onset. About 3 min prior to the substorm onset (Figure 1c) the preexisting arc at ~70° magnetic latitude (MLAT) gradually intensified, forming a wavy structure at ~0401:18 UT, and this aurora did not expand but stayed dim. The ground magnetic field stayed in the quiet time level. As shown in Figure 1d, the second intensification of the auroral arc occurred at 0403:42 UT at 22.2 h MLT, which was located just east of the THEMIS D footprint. This auroral intensification occurred concurrently with an increase (SNKQ) and a decrease (KUUJ) in the X (northward) component of the ground magnetic field of about a few tens of nT, indicating the development of eastward and westward auroral electrojets, respectively. *Pu et al.* [2010] also identified two auroral intensifications, at ~0401:21 and ~0404:30 UT, in this event. By our definition, the second auroral intensification was associated with the substorm onset. After the auroral onset, the aurora then expanded westward and poleward across the footprints of THEMIS D and E (Figures 1e and 1f).

[20] The multistep activations around the auroral breakup (with intervals of several minutes) have been discussed in previous studies [e.g., *Kadokura et al.*, 2002; *Morioka et al.*, 2010; *Saito et al.*, 2010]. They concluded that the stepwise evolution of auroral breakup was likely common. In this event, our focus is the second auroral intensification, which showed the azimuthal expansion of the auroral arc.

[21] Figure 2 summarizes the westward auroral expansion shown in Figure 1. Figure 2a represents an east–west keogram at SNKQ. It represents the average auroral intensity between 67° and 72° MLAT as a function of MLT with ΔMLT of 0.02 h using the ASI. The MLTs of the footprints of THEMIS D (22.1 h MLT, light blue) and E (21.8 h MLT, blue) are overplotted. Figures 2b and 2c show the auroral intensity at three selected MLTs near the footprints of THEMIS D (21.95, 22.05, and 22.1 h MLT) and E (21.7, 21.8, and 21.85 h MLT), respectively. The east–west keogram in Figure 2a shows the azimuthal auroral expansion after the onset at 0403:42 UT as indicated by the white lines, and the aurora expanded westward near the footprints of THEMIS D and E. The vertical lines after the onset in Figures 2b and 2c mark the arrivals of the leading edge of the azimuthally expanding aurora at each MLT near the footprints of THEMIS D and E, respectively. The leading edge is defined as the initiation of a sharp increase in auroral intensity after the onset as marked by the white lines in Figure 2a. As mentioned earlier, there were two intensifications near the footprints, and we focused on

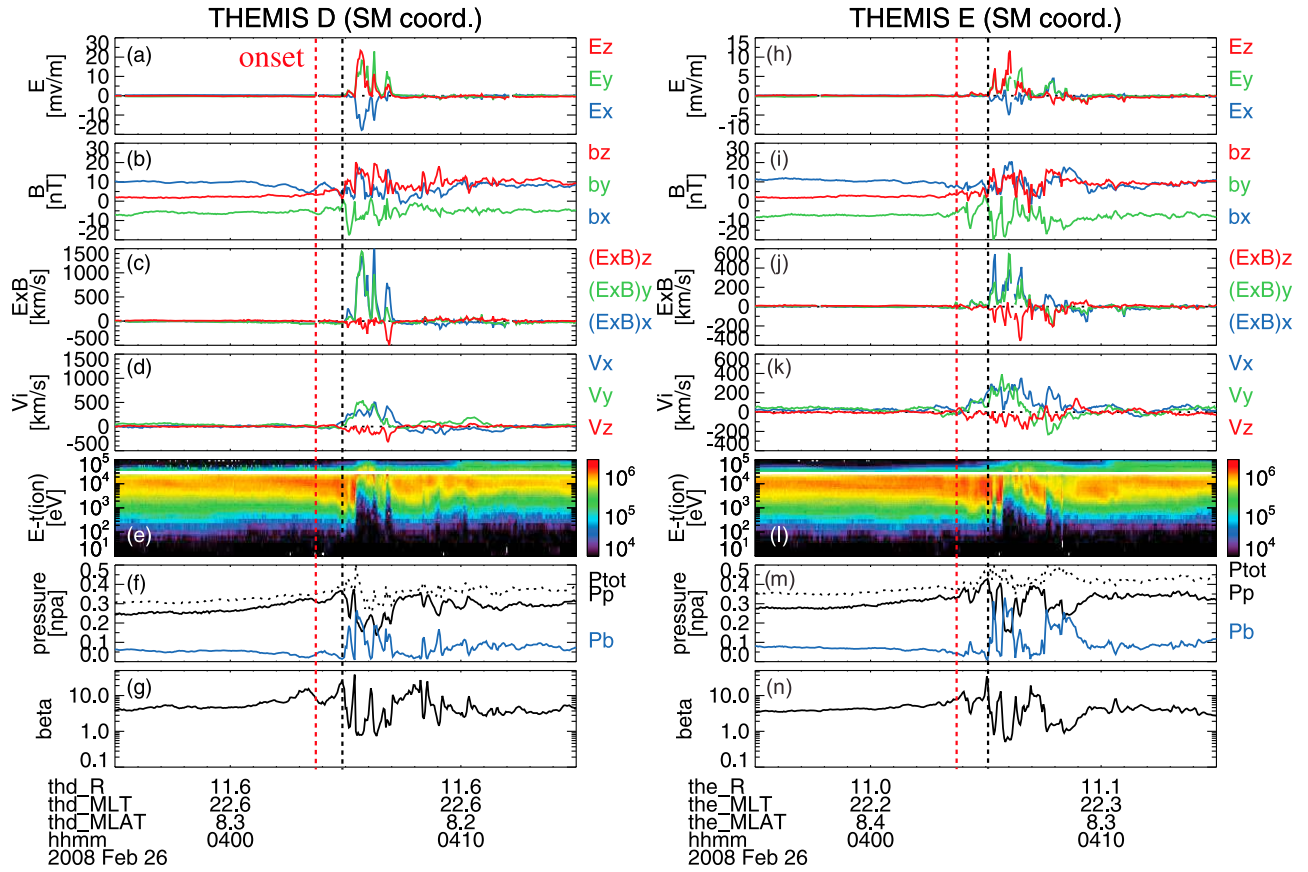

Figure 3. In situ (left) THEMIS D and (right) THEMIS E observations in the near-Earth plasma sheet on 26 February 2008. The vertical red lines mark the auroral onset, 0403:42 UT. The vertical black lines mark the beginning times of magnetic dipolarization at THEMIS D (0404:50 UT) and E (0405:05 UT) locations. (a and h) Electric field assuming $\mathbf{E} \times \mathbf{B} = \mathbf{0}$; (b and i) magnetic field; (c and j) $\mathbf{E} \times \mathbf{B}$ drift speed; (d and k) ion velocity from ESA and SST data; (e and l) ion energy-time spectrogram; (f and m) plasma pressure from ESA and SST (black solid line), magnetic pressure (blue solid line), and total pressure (dashed line); (g and n) ion β. Data in Figures 3a–3d and 3h–3k are given in SM coordinates.

the latter intensification, which expanded azimuthally. The former intensification formed the wavy structure at roughly the same MLT near the THEMIS D footprint, which made it difficult to identify the sharp leading edge of the latter intensification (Figure 2b). We found this ambiguous leading edge near the THEMIS D footprint by comparing the auroral intensity at THEMIS D to the intensity at the THEMIS E footprint; the intensity at the THEMIS E footprint was partially the same as that of the THEMIS D footprint and had a clearer transition of the leading edge. The aurora expanded around the THEMIS D and E footprints by 0.15 h MLT in 15 s and 17 s, respectively. The westward auroral expansion speed of the leading edge was thus 5.6–6.4 km/s.

[22] Figure 3 shows the in situ electromagnetic field and particle data from THEMIS D and E. During the period of the auroral expansion, THEMIS D and E were located at $(-10.6, 4.2, 1.7)\ R_E$ and $(-9.8, 4.9, 1.6)\ R_E$ in SM coordinates, separated by 7074 km. Both spacecraft observed magnetic dipolarization as well as fast azimuthal plasma flows and intense electric fields initiated at the times marked by the vertical black lines. Intensifications of the electric fields correspond to local depletions of the plasma pressure. While a net increase in plasma pressure has often been observed in the inner plasma sheet [e.g., *Miyashita et al.*, 2009; *Xing et al.*, 2010], the local depletion of the plasma pressure that we observed is similar to the one observed in the midtail plasma sheet (~20 R_E), where earthward flows enhance with entropy reduction [e.g., *Sergeev et al.*, 1996].

[23] The possibilities of the observed fast azimuthal plasma flows could be $\mathbf{E} \times \mathbf{B}$ drift flows and pressure gradient–related flows [*Nakamura et al.*, 1999]. It is generally difficult to estimate the spatial gradient, and thus we calculated the approximate upper limit of the azimuthal component of pressure gradient–related flows by assuming that the contribution of the pressure gradient was only the radial direction. This simple calculation gives us a brief estimation for the azimuthal component of pressure gradient flow of ~60 km/s. While the azimuthal component of pressure gradient–related flows is accompanied by the radial and north–south components of pressure gradients, the contribution of the north–south component of the pressure gradient cannot be estimated in our calculation. Hence, we allowed certain errors that stemmed from the formation of the thin current sheet.

[24] In contrast, the plasma flow velocities (Figures 3d and 3k) are generally correlated with the $\mathbf{E} \times \mathbf{B}$ drift speeds (Figures 3c and 3j) within a factor of 2 except for a few spikes

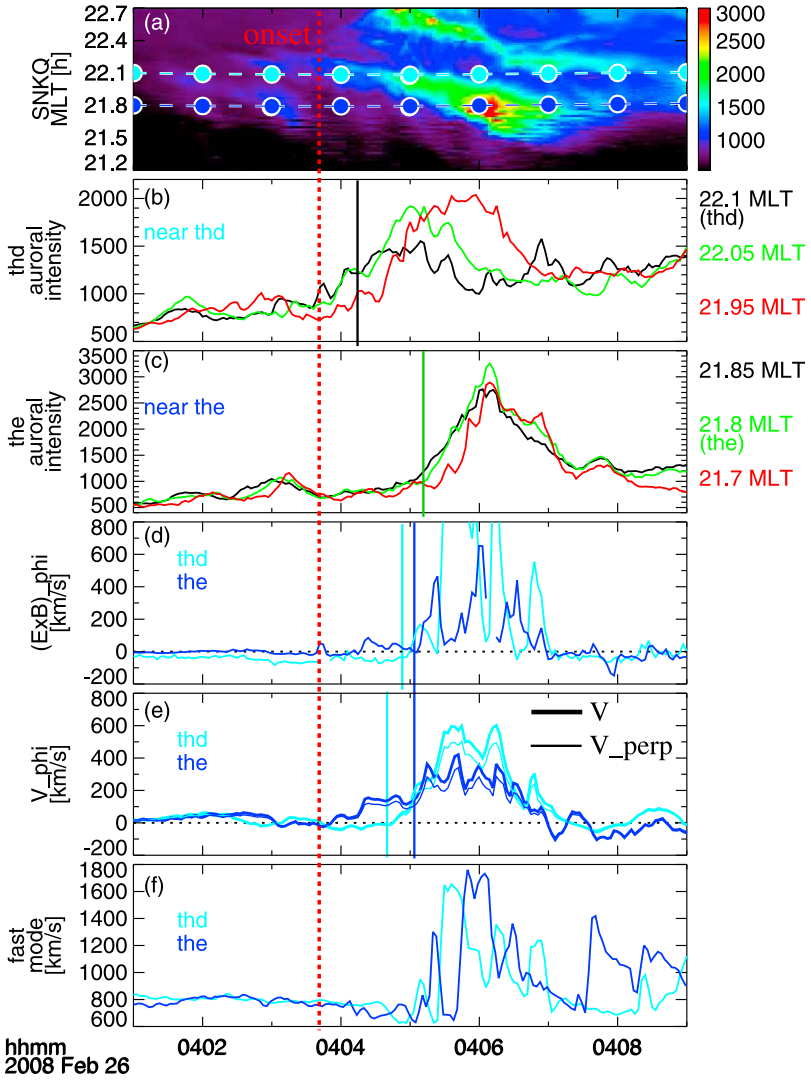

Figure 4. Comparison of ASI and spacecraft data. (a–c) East–west keogram and the line plots of auroral intensity near the footprints of THEMIS D and E. (d and e) The azimuthal component of **E** × **B** drifts and plasma flows, respectively. (f) The phase velocities of the fast-mode wave. In Figures 4d–4f, the light blue line is for THEMIS D, and the blue line is for THEMIS E. In Figure 4e, the thick and thin lines indicate the azimuthal components of plasma flows and their perpendicular components against the magnetic field vector, respectively. The vertical red dashed line marks the auroral onset, 0403:42 UT. The solid vertical lines in Figures 4b and 4c indicate the leading edges of the auroral expansion at the footprints of THEMIS D and E, respectively. The solid blue and light blue lines in Figures 4d and 4e show the initiation of fast azimuthal flows.

in the **E** × **B** drift speeds. The difference in the magnitude of the plasma flows and **E** × **B** drifts, especially during disturbed periods, may be attributed mainly to insufficient calibration of the SST data. (The ion energy spectra in Figures 3d and 3k show significant discontinuity around the energy where the instrument is switched from ESA to SST, so that the SST data can easily be off by a factor of 2 or more.) In particular, the THEMIS E observations show a similar magnitude of ~300 km/s in both the flow moment and the **E** × **B** drift just after the enhancement. This similarity leads us to suggest that the plasma flow at the front of the dipolarization (a permanent B_Z increase) was dominated by the electric drift associated with the intense electric field.

[25] It should be noted that THEMIS E observed the magnetic dipolarization (0405:05 UT) 15 s after it was observed by THEMIS D (0404:50 UT). This time difference corresponds to an approximate westward propagation speed of 470 km/s. Since this propagation speed is comparable to the measured westward plasma flows after the enhancement between ~0405:00 and ~0407:00 UT (Figures 3d and 3k), it suggests that the large-scale structure containing the dipolarization was moving or expanding westward approximately at the measured plasma flow speed during the westward auroral expansion. The qualitative comparison of these speeds is discussed in section 5.

[26] To identify the relationship between the azimuthal auroral expansion and its magnetospheric counterpart, the ASI

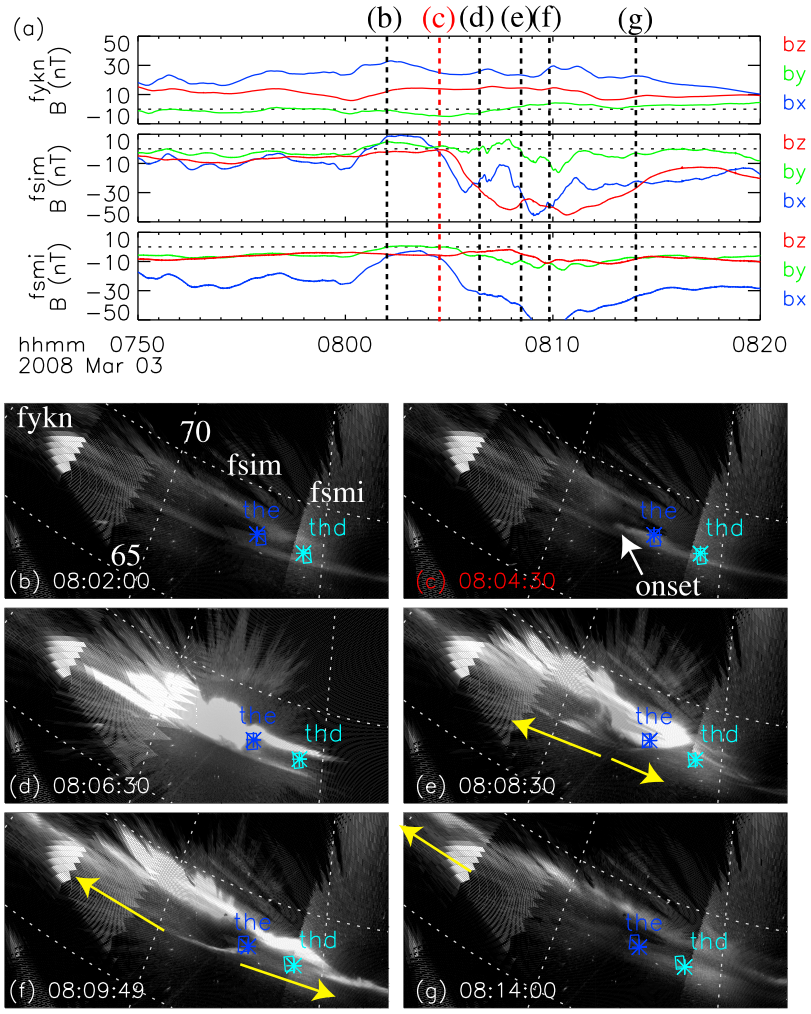

Figure 5. Eastward auroral expansion observed by the ground-based instruments on 3 March 2008. (a) Ground magnetometer data near the footprints of THEMIS D and E. (b–g) Sequence of ASI images at the times of the vertical lines in Figure 6a. All plots in Figures 5b–5g cover magnetic latitudes of ~65–73° in the premidnight sector of ~21–23.5 h MLT. The format is the same as Figure 1.

and spacecraft data are compared in Figure 4. Figures 4a–4c present the east–west keogram and the line plots of the auroral intensity near the footprints (same as those presented in Figure 2). Figures 4d–4f present the azimuthal components of the **E** × **B** drift and plasma flow speeds and the phase velocity of the fast-mode wave derived from the in situ THEMIS D and E data. In Figure 4e, the thick and thin lines indicate the azimuthal components of plasma flows and their perpendicular components against the magnetic field vector, respectively. Since the azimuthal flows and their perpendicular components are nearly the same, we do not distinguish them. The initiation times of the azimuthal plasma flow enhancement (Figure 4e) are roughly consistent with those of the **E** × **B** flow (Figure 4d), while a preceding weak flow was observed by THEMIS E (Figure 4e). Since this weak flow does not appear in the **E** × **B** flow, it may arise from non-MHD processes and may be related to the weak auroral intensification prior to the sharp auroral intensification before the onset.

[27] The identified auroral expansion speed, 5.6–6.4 km/s, corresponds to a speed of 196–235 km/s when mapped to the magnetic equator using the Tsyganenko 96 model. These values are of the same order as the averaged speeds of the azimuthal plasma flows (272–294 km/s), the **E** × **B** drifts (185–309 km/s), and the moving structure deduced from the time difference of the observed dipolarization (~470 km/s). We derived average plasma flow and **E** × **B** drift speeds as the median value from a flow enhancement prior to the flow reversal. The time of the flow enhancement was defined as the start of the magnetic fluctuation (dipolarization). In this event, the time interval selected was ~110 s. The difference between the mapped speed of westward auroral expansion and flow speed detected by the spacecraft would be attributed to the mapping uncertainty of the Tsyganenko 96 model, which does not include substorm time effects. On the other hand, the phase velocity of the fast-mode wave (Figure 4f) is ~1100 km/s, which is much larger than the plasma flow and the mapped auroral expansion speed, indicating that the auroral expansion is not a fast-mode wave propagation but rather plasma transport approximately equal to the **E** × **B** drift speed as mentioned above.

[28] A brief summary of this event is as follows: (1) The leading edge of the westward auroral expansion corresponds

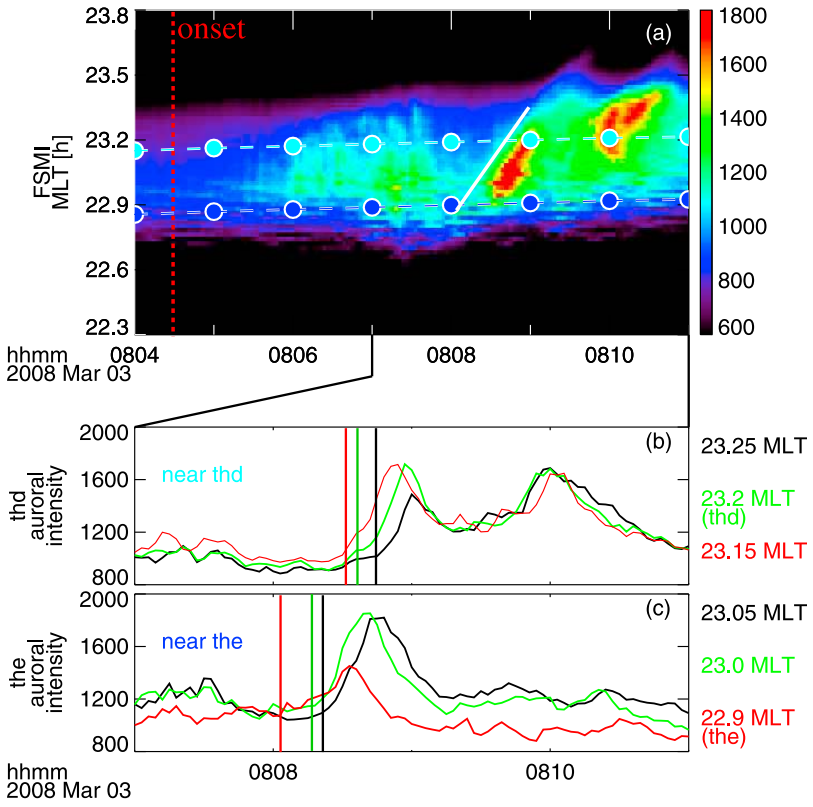

Figure 6. (a) The east–west keogram at FSMI. The MLTs of THEMIS D and E are 23.2 and 22.9 h, respectively. (b) The line plots of auroral intensity at different MLTs near the footprints of THEMIS D (23.15 h MLT, red; 23.2 h MLT, green; and 23.25 h MLT, black). (c) Same near the footprint of THEMIS E. Red, green, and black lines are for 22.9, 23.0, and 23.05 h MLT, respectively. In order to detect the leading edge of the eastward auroral expansion, the time span of Figures 6b and 6c is selected as 4 min. The format is the same as Figure 2.

to the high-speed duskward plasma flow in the magnetosphere, which is associated with the front of the magnetic dipolarization (a steplike B_Z increase) and the intense electric field. (2) The in situ plasma flow moment is mainly composed of the **E** × **B** flow. (3) Because the magnetospheric and ionospheric features were propagating with similar azimuthal speed, it is suggested that magnetospheric disturbance related to the measured large-scale electric field propagated to the ionosphere along the magnetic field line.

3.2. The Eastward Expansion on 3 March 2008

[29] Figure 5 presents the eastward auroral expansion event associated with the auroral onset at 0804:30 UT on 3 March 2008, including ground magnetometer data and a sequence of ASI images obtained at the Fort Yukon (FYKN), Fort Simpson (FSIM), and Fort Smith (FSMI) magnetometers. Before the onset, the magnetic field perturbation was small, and weak east–west aligned arcs appeared (Figure 5b). The entire sequence of images is given in auxiliary material Animation S2. The onset occurred at ~0804:30 UT at 22.8 h MLT and 68° MLAT (Figure 5c), which was located just west of the THEMIS E footprint. At the same time, the X component of the ground magnetic fields at FSIM and FSMI began to decrease by a few tens of nT, indicating the development of a westward auroral electrojet associated with the substorm onset. The onset arc then gradually developed (Figure 5d) and began to expand both eastward and westward at ~0808:30 UT. The aurora was expanding eastward at the footprints of THEMIS D and E (Figures 5e and 5f). We focused not on the gradual intensification at ~0806:00 UT but rather on the second intensification at ~0808:30 UT followed by the fast azimuthal auroral expansion.

[30] Figure 6 summarizes the eastward auroral expansion shown in Figure 5. Figure 6a represents the east–west keogram at FSMI, in which the footprints of THEMIS D (23.2 h MLT, light blue) and E (22.9 h MLT, blue) are overplotted. Figures 6b and 6c show the auroral intensity at three selected MLTs near the footprints of THEMIS D (23.15, 23.2, and 23.25 h MLT) and E (22.9, 23.0, and 23.05 h MLT), respectively. In order to detect the leading edge of the eastward auroral expansion, the time span of Figures 6b and 6c is selected as 4 min. The east–west keogram shows eastward auroral expansion near the footprints (white solid line) associated with a further auroral intensification after the onset. The leading edge of the aurora propagated 0.1 h MLT eastward near the THEMIS D footprint in 13 s and 0.15 h MLT near the THEMIS E footprint in 18 s, which corresponded to an eastward auroral expansion speed of 4.9–5.6 km/s.

[31] The THEMIS D and E observations in the near-Earth plasma sheet are shown in Figure 7. During the period of the auroral expansion, THEMIS D and E were located at (−11.3,

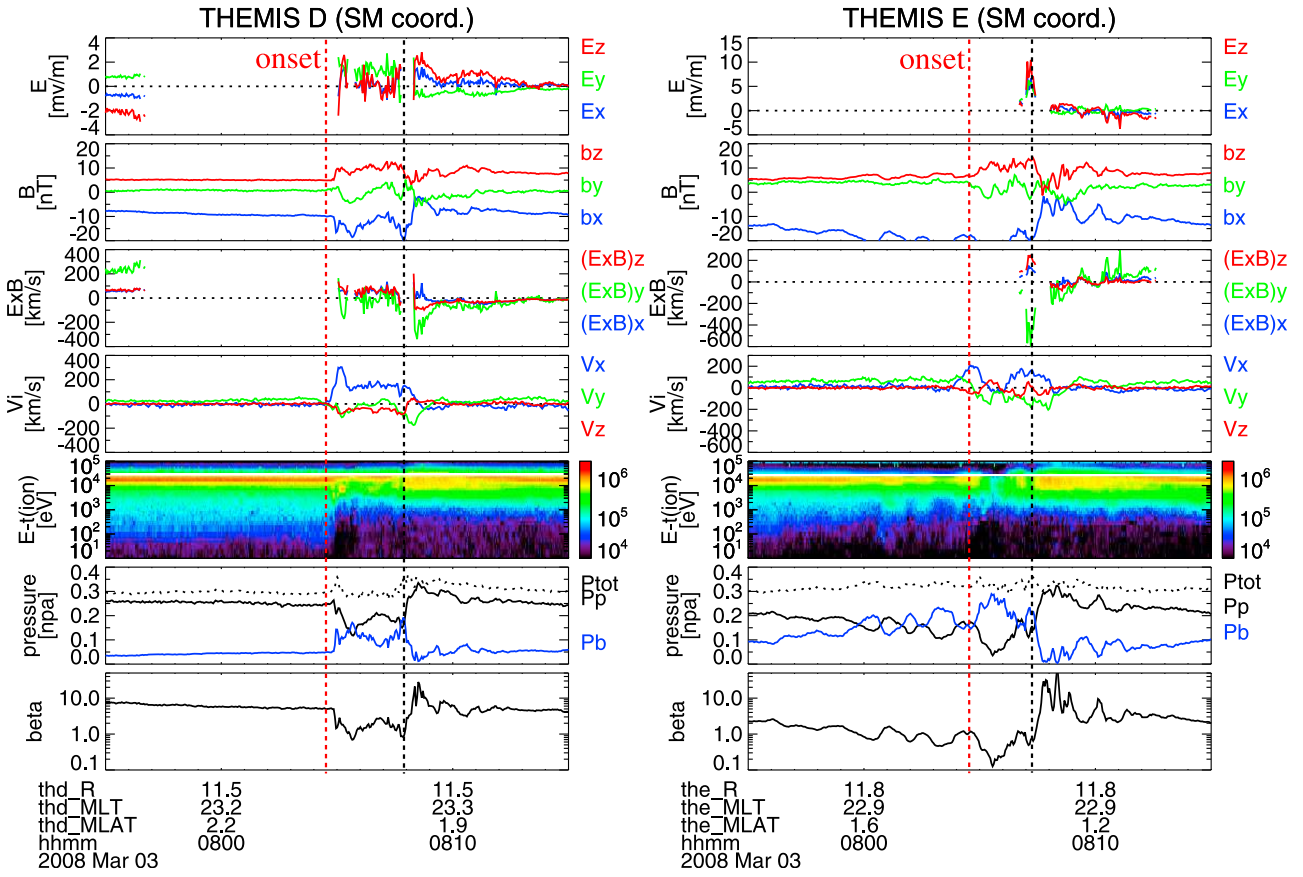

Figure 7. THEMIS D and E observations with 3 s resolution on 3 March 2008. The format is the same as Figure 3.

2.3, 0.5) R_E and (−11.3, 3.3, 0.3) R_E, respectively, in SM coordinates, separated by 6238 km. Both of the spacecraft observed small magnetic dipolarization as well as high-speed earthward and dawnward plasma flows. The third component of the electric field was only intermittently available in this event because of small angles between the spin plane and ambient magnetic field, while the **E** × **B** drift had a variation similar to that of the plasma flow moment. Moreover, the upper limit of pressure gradient–related flows applied in the first event was −30 km/s, smaller than that of the **E** × **B** flows. It should also be noted that both of the spacecraft observed local depletions of the plasma pressure, which were similar to the first event. These similarities suggest that azimuthal plasma transport after the onset was governed by the **E** × **B** drift. After the dipolarization, THEMIS D observed a further decrease in $|B_x|$ associated with the high-speed dawnward flows (0807:20 UT), followed by the THEMIS E detection (0807:55 UT) 35 s later. This time difference corresponds to an eastward propagation speed of 178 km/s. Since this propagation speed was comparable to that of the measured eastward plasma flows shown in Figure 8c, we can thus conclude that the large-scale structure containing the dipolarization was moving eastward approximately at the measured in situ plasma flow speed during the eastward auroral expansion, which was consistent with the westward auroral expansion case (see section 3.1).

[32] Figure 8 presents the east–west keogram, the line plots of auroral intensity near the footprints, the X component of the magnetic field, the azimuthal plasma flows and their perpendicular components against the magnetic field vector, and the phase velocities of the fast-mode wave observed by THEMIS D and E. We plotted B_x in Figure 8d in order to detect the azimuthal plasma flows associated with the dipolarization. The identified auroral expansion speed of 4.9–5.6 km/s corresponds to a speed of 149–171 km/s when mapped to the magnetic equator using the Tsyganenko 96 model. This value is close to the averaged speeds of the dawnward plasma flows (101–105 km/s), **E** × **B** drifts (131–198 km/s), and an eastward moving structure (~178 km/s). The time of the flow enhancement was ~50 s. The phase velocity of the fast-mode wave (~820 km/s) was much larger than that of the plasma flows and the mapped expansion speed, also indicating that the auroral expansion is not a fast-mode wave propagation but rather plasma transport dominated by the **E** × **B** drift. Figure 8 emphasizes that the leading edge of the eastward auroral expansion corresponds to the high-speed dawnward plasma flow and the magnetic dipolarization, as suggested in the westward auroral expansion case.

4. Statistical Study

[33] In this section, we present a statistical analysis of the 16 events that showed azimuthal expansion of auroral arcs selected according to the criteria in section 2. We compared speeds of azimuthal auroral expansion and in situ azimuthal

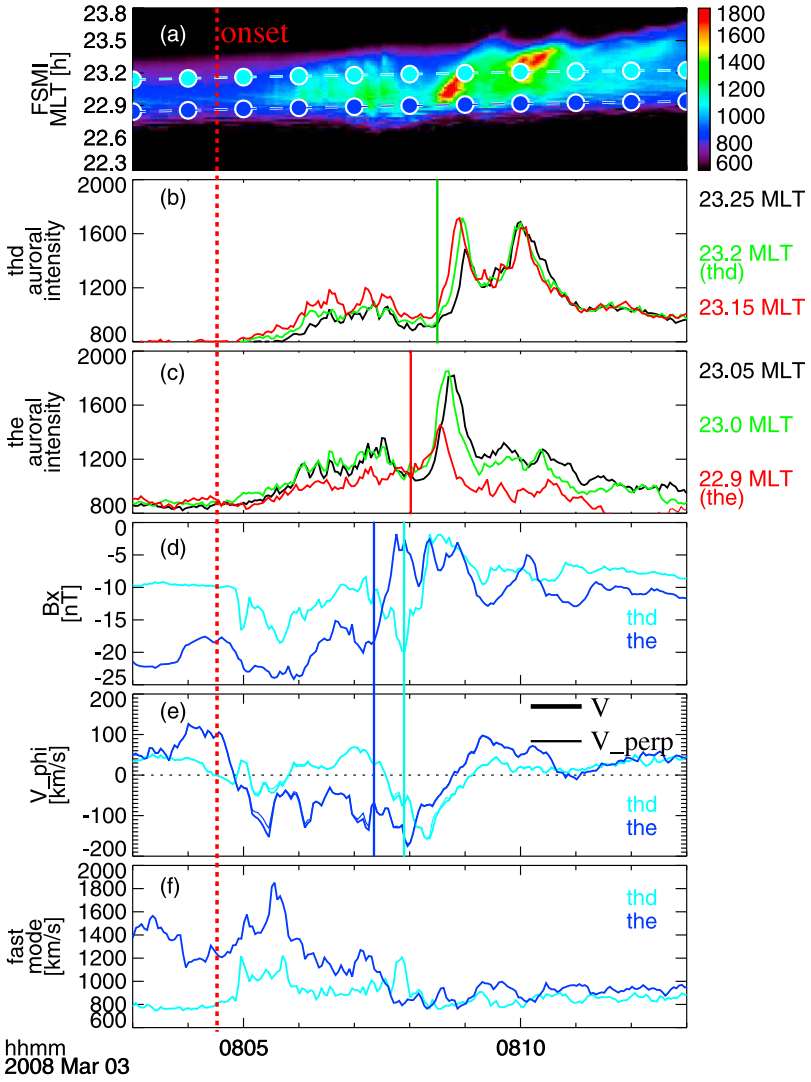

Figure 8. Comparison of the ASI and spacecraft data. (a) The east–west keogram. (b and c) The line plots of auroral intensity near the footprints of THEMIS D and E. (d) The *X* component of the magnetic field. (e) The azimuthal plasma flows (the thick lines) and their perpendicular components against the magnetic field vector (the thin lines). (f) The phase velocities of the fast-mode wave. In Figures 8d–8f, the light blue line is for THEMIS D, and the blue line is for THEMIS E. The vertical red dashed line marks the auroral onset, 0804:30 UT. The solid vertical lines in Figures 8b and 8c indicate the leading edge of the auroral expansion at the footprints of THEMIS D and E, respectively. The solid blue and light blue lines in Figures 8d and 8e show the initiation of fast azimuthal flows related to the decrease in $|B_x|$.

flow associated with magnetic dipolarization. Speeds of azimuthal auroral expansion and in situ azimuthal plasma and **E** × **B** drift flows were calculated from the same method adopted in section 3.

[34] Figure 9 presents the speed of the azimuthal auroral expansion and the averaged speeds of the azimuthal plasma flows (dots) and **E** × **B** drifts (squares) during enhanced flows associated with dipolarization in the near-Earth plasma sheet. The horizontal axes denote the azimuthal auroral expansion speeds at the ionospheric altitude (Figure 9a) and in the equatorial magnetosphere mapped by the Tsyganenko 96 model (Figure 9b). The direction of the plasma flow and **E** × **B** drift velocities is the same as that of the azimuthal auroral expansion. The small difference between the **E** × **B** drift and plasma flow speeds in almost all events could be attributed to insufficient calibration of the SST data.

[35] The speeds of the azimuthal auroral expansion are in a range of 2–15 km/s, which are comparable to those reported in several previous studies on auroral expansion [e.g., *Oguti*, 1973; *Kadokura et al.*, 2002; *Sakaguchi et al.*, 2009]. The average speed of the westward auroral expansion events (8.8 km/s) is larger than that of the eastward expansion events (5.3 km/s). Faster westward expansion implies that the auroral onset tends to occur in the distorted duskside convection cell in the ionosphere, which has westward background plasma flows in the Harang flow shear at the premidnight sector [e.g., *Zou et al.*, 2009]. In our case, the averaged onset MLT was 23.1 h in 11 events (as shown in Table 1), where the onset locations were detected within

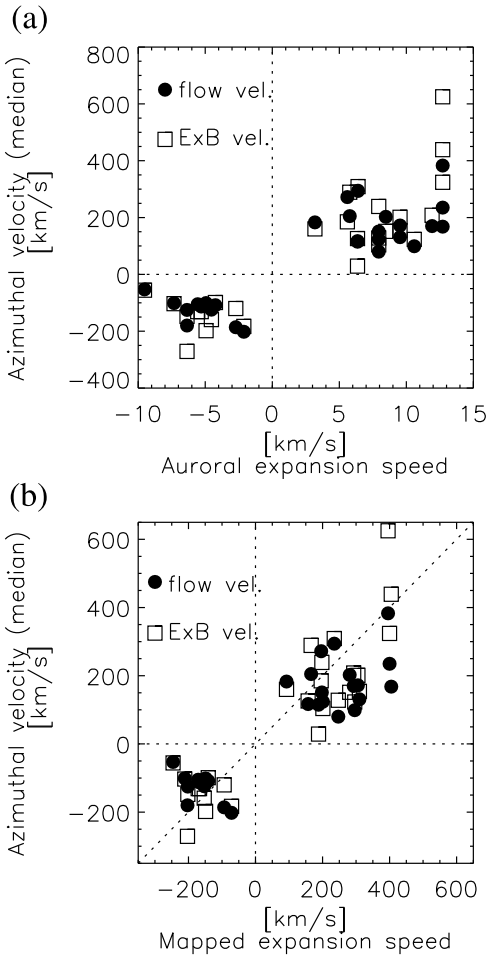

Figure 9. The speeds of the auroral azimuthal expansion derived from ASI data and the in situ azimuthal plasma flow (dots) and **E** × **B** drift (squares) speeds observed by the spacecraft. The horizontal axes denote the azimuthal auroral expansion speed (a) at the ionospheric altitude and (b) in the equatorial magnetosphere mapped by the Tsyganenko 96 model. Positive speeds are westward, and negative speeds are eastward.

the fields of view of ASIs. It is also noted that the duration of the westward auroral expansion was longer than that of the eastward expansion (not shown). The east–west asymmetry in the auroral expanding speed and duration suggests that the development of the azimuthally expanding aurora may depend on the onset location in terms of the pattern and strength of large-scale ionospheric convection.

[36] The speeds of azimuthal auroral expansion (8.8 km/s and 5.3 km/s) were found to be 267 km/s and 162 km/s when mapped onto the magnetosphere at the equatorial plane. These speeds are comparable to the averaged speeds of the enhanced in situ azimuthal flow observed by the spacecraft, that is, 193 km/s (plasma flow) and 239 km/s (**E** × **B** drift) in the westward direction and 112 km/s (plasma flow) and 139 km/s (**E** × **B** drift) in the eastward direction, including the agreement in the east–west asymmetry. The east–west asymmetry of the propagation speed was also confirmed in the magnetosphere [*Hori et al.*, 2000; *Kaufmann et al.*, 2001; *Liou et al.*, 2002]. *Liou et al.* [2002] showed that the westward expansion speed of the dipolarization region at the geosynchronous orbit (~75 km/s) was larger than the eastward speed (~60 km/s). While *Liou et al.* [2002] detected the east–west asymmetry in the expansion speed of the dipolarization far from the onset region, we found it for the first time near the onset region in the near-Earth plasma sheet along with the asymmetry in the azimuthal auroral expansion. Since the magnetospheric and ionospheric structures propagated azimuthally at a similar speed, we can conclude that the azimuthal auroral expansion is closely related to the magnetic dipolarization in the near-Earth plasma sheet which expands azimuthally at the measured azimuthal plasma flow speed.

[37] *Hori et al.* [2000] suggested that the asymmetry of a magnetospheric convection was due to the non-MHD drift (pressure gradient–related flow) in the average sense, which is directed westward for ions, while the **E** × **B** drift was quite symmetric in the noon-midnight meridian. In the present study, we found that the calculated **E** × **B** drifts as well as plasma bulk flow tended to be larger in the westward direction during substorms, suggesting that the east–west asymmetries of flow patterns were mainly accompanied by the MHD process because of the presence of intense electric fields, which would be significantly intensified in the western part of the onset region as compared to the east region.

5. Discussion

[38] Fast azimuthal plasma flows in the near-Earth plasma sheet have been detected in past studies [e.g., *Yeoman et al.*, 1998; *Nakamura et al.*, 1999; *Angelopoulos et al.*, 2008b]. Using a network of ground magnetometers, *Yeoman et al.* [1998] showed an azimuthal ionospheric feature propagating eastward with a speed of ~6 km/s that was associated with magnetic dipolarization and fast dawnward plasma flow observed by the Geotail spacecraft located in the near-Earth plasma sheet ~4 h MLT to the east of the ionospheric disturbances. In the present study, for the first time we have investigated an auroral feature expanding azimuthally near the magnetic footprints of near-Earth spacecraft and have shown that the magnetic dipolarization and fast azimuthal flows in the near-Earth plasma sheet are closely associated with the azimuthal auroral expansion. The east–west asymmetry of azimuthally propagation speeds in both the magnetosphere and the ionosphere also supported their close relationship.

[39] There are mainly two explanations for the observed fast azimuthal flows: a braking process of bursty bulk flows generated by nightside reconnection [e.g., *Shiokawa et al.*, 1997, 1998] and the development of near-Earth instabilities [e.g., *Lui*, 1996; *Liang et al.*, 2005, 2008]. It can be suggested that the observed fast azimuthal flows are similar to the flow patterns in the near-Earth plasma sheet that were recently observed using mainly the THEMIS spacecraft [*Keika et al.*, 2009; *Keiling et al.*, 2009; *Ohtani et al.*, 2009; *Panov et al.*, 2010a, 2010b]. For example, *Panov et al.* [2010b] showed by means of five THEMIS probes covering radial distances between 15 R_E and 9 R_E that the fast earthward flow in the magnetotail was largely deflected and reversed its direction tailward because of the increase in the radial pressure gradient. Their results are consistent with the model of the braking

process of bursty bulk flows, which could explain the observed fast azimuthal flows in the present study.

[40] On the other hand, *Saito et al.* [2008] focused on the development of the ballooning instability 1–4 min prior to magnetic dipolarization in the near-Earth plasma sheet. They showed that the low-frequency wave began to be seen a few minutes before the dipolarization in a high plasma beta condition. Its phase velocity should be nearly equal to the azimuthal component of the ambient plasma velocity (a few tens of km/s), so that the wavelength of the wave mode was found to be of the order of the ion Lamor radius. In our first event in section 3, the ballooning-type development was seen by ASI data at ~0358:00 UT and intensified at ~0401:18 UT, when the magnetic and plasma signatures were weak. These signatures are thought to be the same disturbances reported by *Saito et al.* [2008]. Thus, the saturation of the ballooning mode could possibly lead to the azimuthal expansion of the onset region. A current sheet instability can also explain fast azimuthal propagation. *Liu and Liang* [2009] performed a two-fluid MHD simulation of a current sheet instability which predicted an azimuthal speed of ~250 km/s of current disruption.

[41] We observed intense electric fields associated with magnetic dipolarization and auroral expansion. Such electric fields tend to be observed with dipolarization [*Birn and Hesse*, 1996; *Tu et al.*, 2000; *Ohtani et al.*, 2007; *Nishimura et al.*, 2008]. It is not possible to determine from the present observations whether the observed electric fields were electrostatic or inductive. Our finding that the magnetospheric and auroral features were propagating azimuthally at a similar speed indicates that the intense electric fields detected in the near-Earth plasma sheet would be connected to the ionosphere through Alfvén waves along magnetic field lines. This may suggest the presence of large electrostatic fields, but we cannot rule out the possibility of inductive fields since the current observation points are not sufficient to estimate $\nabla \times \mathbf{E}$ and inductive electric fields may modify electrostatic fields [cf. *Heikkila and Pellinen*, 1977]. Moreover, a two-dimensional particle simulation showed that the thin current sheet in the magnetotail generally requires an electrostatic potential which is closed through parallel electric fields at the auroral acceleration region [*Birn et al.*, 2004]. This study cannot estimate the magnitude of parallel potential drop, which might lead to decoupling between the ionosphere and magnetosphere. Such electric fields are suggested to be related to substorm onset turbulence, although the present study does not give information about the mechanism itself.

[42] This fast auroral feature has rarely been observed using radars, which typically have a spatial and time resolution of ~50 km and 1–2 min, respectively. Since we focused on the leading edge of azimuthal auroral expansion and its spatial scale was smaller than the typical spatial resolution of radars, the auroral leading edge would propagate more than several spatial grid sizes of radars during the observation cadence. Thus, we think that velocity observations currently available from radar observations would be insufficient and only represent averaged flows in larger spatial and time scales than those of a single auroral arc propagating much faster than the background. Moreover, during large auroral intensifications, echoes from the ionosphere detected by coherent radars tend to disappear because of the absorption of the radio waves. These would make it difficult to detect fast azimuthally propagating features in the ionosphere. Although the velocity measured by radars tends to be smaller than that of auroral motion, a few radar observations suggested the existence of fast azimuthal flow bursts in the auroral ionosphere with speeds of 1–2 km/s [*Walker et al.*, 1998; *Senior et al.*, 2002]. Further studies using radar observations of ionospheric electric fields should be conducted to provide additional direct evidence of the electrostatic nature of electric fields.

6. Conclusions

[43] In the present paper, we have adopted coordinated observations of the THEMIS all-sky imagers and multiple spacecraft for the investigation of azimuthal auroral expansion associated with magnetic dipolarization. For the first time, we detected the azimuthal expansion of auroral arcs that passed near the magnetic footprints of the multiple spacecraft operating in the near-Earth plasma sheet, using high spatiotemporal auroral observations.

[44] During azimuthal auroral expansion at the footprint locations, the multiple THEMIS spacecraft frequently observed fast azimuthal flows and intense electric fields as well as magnetic dipolarization. The time differences of the observed dipolarization among the multiple spacecraft indicated that a large-scale structure propagated azimuthally with a speed close to the measured in situ plasma flow speed. The plasma flow speed was dominated by the $\mathbf{E} \times \mathbf{B}$ drift associated with the dipolarization and intense electric fields. Two event studies commonly suggest that the leading edge of the azimuthal auroral expansion corresponds to the fast azimuthal plasma flow, which is associated with the front of the magnetic dipolarization and intense electric field.

[45] We performed statistical analyses of the selected 16 events that showed azimuthal auroral expansion associated with magnetic dipolarization in the near-Earth plasma sheet. The results showed that the speeds of the azimuthal auroral expansion in the ionosphere and the plasma flow and $\mathbf{E} \times \mathbf{B}$ drift in the magnetosphere had east–west asymmetry, i.e., that it was faster in the westward direction. The averaged speeds of the azimuthal auroral expansion were 8.8 km/s (westward) and 5.3 km/s (eastward). When mapped onto the equatorial plane, these speeds (267 km/s and 162 km/s) were comparable to the averaged azimuthal speeds observed by the spacecraft (193–239 km/s westward and 112–139 km/s eastward). A faster westward propagation in the ionosphere and magnetosphere implies that the auroral onset tends to occur in the distorted duskside convection cell in the ionosphere, which has westward background convection in the Harang flow shear at the premidnight sector.

[46] We detected intense electric fields in the near-Earth plasma sheet associated with auroral expansion. The auroral motion approximately at the $\mathbf{E} \times \mathbf{B}$ flow speed suggests that the effects of the intense, large-scale electric fields, which are possibly generated through substorm onset turbulence, propagate toward the ionosphere along the magnetic field lines and lead to azimuthal expansion of an auroral arc.

[47] **Acknowledgments.** This work was supported by the Tohoku University Global COE program "Global Education and Research Center for Earth and Planetary Dynamics" and the JSPS Research Fellowships for

Young Scientists. The THEMIS project is funded by NASA contract NAS5-02099. The deployment of the THEMIS ASIs was partly supported by CSA contract 9F007-046101. OMNI solar wind data were provided through the Coordinated Data Analysis Web. We are deeply thankful to J. McFadden for providing the THEMIS ESA data. K.O. and Y.K. express thanks to M. Fujimoto for the assistance and coordination between the Japanese community and the THEMIS project.

[48] Robert Lysak thanks Victor Sergeev and another reviewer for their assistance in evaluating this paper.

References

Akasofu, S.-I. (1964), The development of the auroral substorm, *Planet. Space Sci.*, *12*, 273–282, doi:10.1016/0032-0633(64)90151-5.

Angelopoulos, V. (2008), The THEMIS mission, *Space Sci. Rev.*, *141*, 5–34, doi:10.1007/s11214-008-9336-1.

Angelopoulos, V., et al. (2008a), Tail reconnection triggering substorm onset, *Science*, *321*, 931–935, doi: 10.1126/science.1160495.

Angelopoulos, V., et al. (2008b), First results from the THEMIS mission, *Space Sci. Rev.*, *141*, 453–476, doi: 10.1007/s11214-008-9378-4.

Auster, H. U., et al. (2008), The THEMIS Fluxgate Magnetometer, *Space Sci. Rev.*, *141*, 235–264, doi:10.1007/s11214-008-9365-9.

Birn, J., and M. Hesse (1996), Details of current disruption and diversion in simulations of magnetotail dynamics, *J. Geophys. Res.*, *101*(A7), 15,345–15,358, doi:10.1029/96JA00887.

Birn, J., K. Schindler, and M. Hesse (2004), Thin electron current sheets and their relation to auroral potentials, *J. Geophys. Res.*, *109*, A02217, doi:10.1029/2003JA010303.

Bonnell, J. W., F. S. Mozer, G. T. Delory, A. J. Hull, R. E. Ergun, C. M. Cully, V. Angelopoulos, and P. R. Harvey (2008), The Electric Field Instrument (EFI) for THEMIS, *Space Sci. Rev.*, *141*, 303–341, doi:10.1007/s11214-008-9469-2.

Heikkila, W. J., and R. J. Pellinen (1977), Localized induced electric field within the magnetotail, *J. Geophys. Res.*, *82*(10), 1610–1614, doi:10.1029/JA082i010p01610.

Hori, T., K. Maezawa, Y. Saito, and T. Mukai (2000), Average profile of ion flow and convection electric field in the near-Earth plasma sheet, *Geophys. Res. Lett.*, *27*(11), 1623–1626, doi:10.1029/1999GL003737.

Kadokura, A., A.-S. Yukimatu, M. Eriji, T. Oguti, M. Pinnock, and P. R. Sutcliffe (2002), Detailed analysis of a substorm event on 6 and 7 June 1989: 2. Stepwise auroral bulge evolution during expansion phase, *J. Geophys. Res.*, *107*(A12), 1480, doi:10.1029/2001JA009129.

Kaufmann, R. L., B. M. Ball, W. R. Paterson, and L. A. Frank (2001), Plasma sheet thickness and electric currents, *J. Geophys. Res.*, *106*(A4), 6179–6193, doi:10.1029/2000JA000284.

Keika, K., et al. (2009), Observations of plasma vortices in the vicinity of flow-braking: A case study, *Ann. Geophys.*, *27*, 3009–3017, doi:10.5194/angeo-27-3009-2009.

Keiling, A., et al. (2009), Substorm current wedge driven by plasma flow vortices: THEMIS observations, *J. Geophys. Res.*, *114*, A00C22, doi:10.1029/2009JA014114.

Kubyshkina, M., V. Sergeev, N. Tsyganenko, V. Angelopoulos, A. Runov, H. Singer, K. H. Glassmeier, H. U. Auster, and W. Baumjohann (2009), Toward adapted time-dependent magnetospheric models: A simple approach based on tuning the standard model, *J. Geophys. Res.*, A00C21, *114*, doi:10.1029/2008JA013547.

Liang, J., E. F. Donovan, G. J. Sofko, and T. Trondsen (2005), Substorm dynamics revealed by ground observations of two-dimensional auroral structures on 9 October 2000, *Ann. Geophys.*, *23*, 3599–3613, sref:1432-0576/ag/2005-23-3599.

Liang, J., E. F. Donovan, W. W. Liu, B. Jackel, M. Syrjäsuo, S. B. Mende, H. U. Frey, V. Angelopoulos, and M. Connors (2008), Intensification of preexisting auroral arc at substorm expansion phase onset: Wave-like disruption during the first tens of seconds, *Geophys. Res. Lett.*, *35*, L17S19, doi:10.1029/2008GL033666.

Liou, K., C.-I. Meng, A. T. Y. Lui, P. T. Newell, and S. Wing (2002), Magnetic dipolarization with substorm expansion onset, *J. Geophys. Res.*, *107*(A7), 1131, doi:10.1029/2001JA000179.

Liu, W. W., and J. Liang (2009), Disruption of magnetospheric current sheet by quasi-electrostatic field, *Ann. Geophys.*, *27*, 1941–1950, doi:10.5194/angeo-27-1941-2009.

Lopez, R. E., D. G. Sibeck, R. W. McEntire, and S. M. Krimigis (1990), The energetic ion substorm injection boundary, *J. Geophys. Res.*, *95*(A1), 109–117, doi:10.1029/JA095iA01p00109.

Lui, A. T. Y. (1996), Current disruption in the Earth's magnetosphere: Observations and models, *J. Geophys. Res.*, *101*(A6), 13,067–13,088, doi:10.1029/96JA00079.

McFadden, J. P., C. W. Carlson, D. Larson, M. Ludlam, R. Abiad, B. Elliott, P. Turin, M. Marckwordt, and V. Angelopoulos (2008), The THEMIS ESA plasma instrument and in-flight calibration, *Space Sci. Rev.*, *141*, 277–302, doi:10.1007/s11214-008-9440-2.

McPherron, R. L., C. T. Russell, and M. P. Aubry (1973), Satellite studies of magnetospheric substorms on August 15, 1968: 9. Phenomenological model for substorms, *J. Geophys. Res.*, *78*(16), 3131–3149, doi:10.1029/JA078i016p03131.

Mende, S. B., S. E. Harris, H. U. Frey, V. Angelopoulos, C. T. Russell, E. Donovan, B. Jackel, M. Greffen, and L. M. Peticolas (2008), The THEMIS array of ground-based observatories for the study of auroral substorms, *Space Sci. Rev.*, *141*, 357–387, doi:10.1007/s11214-008-9380-x.

Miyashita, Y., et al. (2009), A state-of-the-art picture of substorm-associated evolution of the near-Earth magnetotail obtained from superposed epoch analysis, *J. Geophys. Res.*, *114*, A01211, doi:10.1029/2008JA013225.

Morioka, A., et al. (2010), Two-step evolution of auroral acceleration at substorm onset, *J. Geophys. Res.*, *115*, A11213, doi:10.1029/2010JA015361.

Nagai, T. (1982), Observed magnetic substorm signatures at synchronous altitude, *J. Geophys. Res.*, *87*(A6), 4405–4417, doi:10.1029/JA087iA06p04405.

Nagai, T., D. N. Baker, and P. R. Higbie (1983), Development of substorm activity in multiple-onset substorms at synchronous orbit, *J. Geophys. Res.*, *88*(A9), 6994–7004, doi:10.1029/JA088iA09p06994.

Nakamura, R., T. Oguti, T. Yamamoto, and S. Kokubun (1993), Equatorward and poleward expansion of the auroras during auroral substorms, *J. Geophys. Res.*, *98*(A4), 5743–5759, doi:10.1029/92JA02230.

Nakamura, R., et al. (1999), Substorm observations in the early morning sector with Equator-S and Geotail, *Ann. Geophys.*, *17*, 1602–1610, doi:10.1007/s00585-999-1602-3.

Nishimura, Y., J. Wygant, T. Ono, M. Iizima, A. Kumamoto, D. Brautigam, and F. Rich (2008), Large-amplitude wave electric field in the inner magnetosphere during substorms, *J. Geophys. Res.*, *113*, A07202, doi:10.1029/2007JA012833.

Nishimura, Y., L. Lyons, S. Zou, V. Angelopoulos, and S. Mende (2010), Substorm triggering by new plasma intrusion: THEMIS all-sky imager observations, *J. Geophys. Res.*, *115*, A07222, doi:10.1029/2009JA015166.

Oguti, T. (1973), Hydrogen emission and electron aurora at the onset of the auroral breakup, *J. Geophys. Res.*, *78*(31), 7543–7547, doi:10.1029/2009JA078i031p07543.

Ohtani, S., et al. (2007), Cluster observations in the inner magnetosphere during the 18 April 2002 sawtooth event: Dipolarization and injection at $r = 4.6\ R_E$, *J. Geophys. Res.*, *112*, A08213, doi:10.1029/2007JA012357.

Ohtani, S., Y. Miyashita, H. Singer, and T. Mukai (2009), Tailward flows with positive B_Z in the near-Earth plasma sheet, *J. Geophys. Res.*, *114*, A06218, doi:10.1029/2009JA014159.

Panov, E. V., et al. (2010a), Multiple overshoot and rebound of a bursty bulk flow, *Geophys. Res. Lett.*, *37*, L08103, doi:10.1029/2009GL041971.

Panov, E. V., et al. (2010b), Plasma sheet thickness during a bursty bulk flow reversal, *J. Geophys. Res.*, *115*, A05213, doi:10.1029/2009JA014743.

Pu, Z. Y., et al. (2010), THEMIS observations of substorms on 26 February 2008 initiated by magnetotail reconnection, *J. Geophys. Res.*, *115*, A02212, doi:10.1029/2009JA014217.

Pytte, T., R. L. McPherron, and S. Kokubun (1976), The ground signatures of the expansion phase during multiple onset substorms, *Planet. Space Sci.*, *24*, 1115–1132, doi:10.1016/0032-0633(76)90149-5.

Saito, M. H., Y. Miyashita, M. Fujimoto, I. Shinohara, Y. Saito, K. Liou, and T. Mukai (2008), Ballooning mode waves prior to substorm-associated dipolarizations: Geotail observations, *Geophys. Res. Lett.*, *35*, L07103, doi:10.1029/2008GL033269.

Saito, M. H., Y. Miyashita, M. Fujimoto, K. Liou, Y. Saito, and J. B. Sigwarth (2010), Stepwise feature of aurora during substorm expansion compared with the near-Earth tail dipolarizations: Possible types of substorm dynamics, *J. Geophys. Res.*, *115*, A02207, doi:10.1029/2009JA014572.

Sakaguchi, K., K. Shiokawa, A. Ieda, R. Nomura, A. Nakajima, M. Greffen, E. Donovan, I. R. Mann, H. Kim, and M. Lessard (2009), Fine structures and dynamics in auroral initial brightening at substorm onsets, *Ann. Geophys.*, *27*, 623–630, doi:10.5194/angeo-27-623-2009.

Senior, C., J.-C. Cerisier, F. Rich, M. Lester, and G. K. Parks (2002), Strong sunward propagating flow bursts in the night sector during quiet solar wind conditions: SuperDARN and satellite observations, *Ann. Geophys.*, *20*, 771–779, doi:10.5194/angeo-20-771-2002.

Sergeev, V. A., V. Angelopoulos, J. T. Gosling, C. A. Cattell, and C. T. Russell (1996), Detection of localized, plasma-depleted flux tubes or bubbles in the midtail plasma sheet, *J. Geophys. Res.*, *101*(A5), 10,817–10,826, doi:10.1029/96JA00460.

Shiokawa, K., W. Baumjohann, and G. Haerendel (1997), Braking of high-speed flows in the near-Earth tail, *Geophys. Res. Lett.*, *24*(10), 1179–1182, doi:10.1029/97GL01062.

Shiokawa, K., et al. (1998), High-speed ion flow, substorm current wedge, and multiple Pi 2 pulsations, *J. Geophys. Res.*, *103*(A3), 4491–4507, doi:10.1029/97JA01680.

Shiokawa, K., et al. (2009), Longitudinal development of a substorm brightening arc, *Ann. Geophys.*, *27*, 1935–1940, doi:10.5194/angeo-27-1935-2009.

Tsyganenko, N. A. (1995), Modeling the Earth's magnetospheric magnetic field confined within a realistic magnetopause, *J. Geophys. Res.*, *100*(A4), 5599–5612, doi:10.1029/94JA03193.

Tu, J.-N., K. Tsuruda, H. Hayakawa, A. Matsuoka, T. Mukai, I. Nagano, and S. Yagitani (2000), Statistical nature of impulsive electric fields associated with fast ion flow in the near-Earth plasma sheet, *J. Geophys. Res.*, *105*(A8), 18,901–18,907, doi:10.1029/1999JA000428.

Uritsky, V. M., J. Liang, E. Donovan, E. Spanswick, D. Knudsen, W. Liu, J. Bonnell, and K. H. Glassmeier (2009), Longitudinally propagating arc wave in the pre-onset optical aurora, *Geophys. Res. Lett.*, *36*, L21103, doi:10.1029/2009GL040777.

Walker, A. D. M., M. Pinnock, K. B. Baker, J. R. Dudeney, and J. P. S. Rash (1998), Strong flow bursts in the nightside ionosphere during extremely quiet solar wind conditions, *Geophys. Res. Lett.*, *25*(6), 881–884, doi:10.1029/98GL00408.

Xing, X., L. R. Lyons, V. Angelopoulos, D. Larson, C. Carlson, A. Runov, and U. Auster (2010), Plasma sheet pressure evolution related to substorms, *J. Geophys. Res.*, *115*, A01212, doi:10.1029/2009JA014315.

Yeoman, T. K., T. Mukai, and T. Yamamoto (1998), Simultaneous ionospheric and magnetospheric observations of azimuthally propagating transient features during substorms, *Ann. Geophys.*, *16*, 754–763, doi:10.1007/s00585-998-0754-x.

Zou, S., L. R. Lyons, M. J. Nicolls, C. J. Heinselman, and S. B. Mende (2009), Nightside ionospheric electrodynamics associated with substorms: PFISR and THEMIS ASI observations, *J. Geophys. Res.*, *114*, A12301, doi:10.1029/2009JA014259.

V. Angelopoulos, Institute of Geophysics and Planetary Physics, University of California, 3845 Slichter Hall, Los Angeles, CA 90095, USA.

J. Bonnell and S. B. Mende, Space Sciences Laboratory, University of California, 7 Gauss Way, Berkeley, CA 94720, USA.

T. Hori, Y. Miyashita, and Y. Nishimura, Solar-Terrestrial Environment Laboratory, Nagoya University, Furo-cho, Chikusa-ku, Nagoya, Aichi 464-8601, Japan.

Y. Kasaba and K. Ogasawara, Department of Geophysics, Tohoku University, Aramaki-Aza Aoba 6-3, Aoba-ku, Sendai, Miyagi 980-8578, Japan. (kasaba@pat.gp.tohoku.ac.jp; k_oga@pat.gp.tohoku.ac.jp)

T. Takada, Department of Electrical Engineering and Information Science, Kochi National College of Technology, Monobe-Otsu 200-1, Nankoku-shi, Kochi 783-8508, Japan.